



OPEN

Landscape change patterns at three stages of the construction and operation of the TGP

Ruikang Li¹, Yangbing Li^{2,3}, Bo Li^{1✉} & Dianji Fu⁴

Analyses of landscape change patterns that are based on elevation and slope can not only provide reasonable interpretations of landscape patterns but can also help to reveal evolutionary laws. However, landscape change patterns and their model in different landforms of the typical watershed in the Three Gorges Reservoir Area (TGRA) has not been quantified and assessed effectively. As a complex geographical unit, the ecological environment in the middle reach of the Yangtze River has experienced great changes due to the construction of the Three Gorges Project (TGP) and its associated human activities. Here, based mainly on a digital elevation model (DEM) and remotely sensed images from 1986, 2000, 2010, and 2017 and by using GIS technology, speeds/ trends of landscape change, the index of landscape type change intensity, landscape pattern indices, and landscape ecological security index, the spatial and temporal evolution characteristics of different elevations, slopes, and buffer landscape types were analyzed in typical watersheds, as well as an evolutionary model of the landscape pattern. The results indicated that (1) the landscape types along with the land classification and buffer zone that were influenced by the TGR construction have undergone a phased change, with the period 2000–2010 being the most dramatic period of landscape evolution during the impoundment period; (2) landscape type shifts from human-dominated farmland to nature-driven forestland and shrub-land as elevations, slopes and buffer distances increased. The landscape has shifted from diversity to relative homogeneity; (3) land types and buffer zones played essential roles in the landscape pattern index, which is reflected in the differences in landscape type indices for spatial extension and temporal characteristics. The results of this paper illustrate the spatial-temporal characteristics of various landscape types at three distinct stages in the construction of the TGR. These findings indicate that the landscape ecological security of the watershed is improving year by year. The follow-up development of the TGRA needs to consider the landscape change patterns of different landforms.

More than 58,000 massive reservoirs had been built worldwide by 2015¹ and approximately 45% of these had been constructed in China². As an effective method for water resource utilization and regulation, dams have made important contributions to social and economic development. More rivers have been altered, and large-scale water conservation projects^{3,4} have been undertaken to satisfy the demands of rapid socioeconomic development^{5,6}. As the greatest contributors to alter rivers' natural properties, the construction of dams causing certain duress on watershed ecosystems to some extent, which can affect landscape distributions by impounding water for prolonged periods. The construction and operation of large reservoirs have profoundly changed the delivery of riverine material⁷, such as causing fragmentation of fish habitats, altering regional climatic environments, resulting in loss of species diversity, increasing soil erosion, and shifting the reservoir's area water levels rhythm, and have caused unprecedented ecological and environmental challenges upstream and downstream⁸. In particular, the construction of master engineering has profoundly influenced landscapes. In recent decades, these changes have attracted extensive attention from experts and scholars around the world^{9–12}. As especially frequent human activities, land inundation, flow manipulation, and fragmentation triggered by reservoir construction¹³ have crucial environmental impacts: unavoidable crop production losses¹⁴, changes in hydrological conditions¹⁵, soil erosion¹⁶, increases in population and pollution inputs¹⁷, which ultimately lead to changes in landscape

¹Faculty of Geographical Science, Beijing Normal University, Beijing 100875, China. ²College of Geography and Tourism, Chongqing Normal University, Chongqing 401331, China. ³Key Laboratory of Surface Process and Environment Remote Sensing in the Three Gorges Reservoir Area, Chongqing Normal University, Chongqing 401331, China. ⁴The Research Center of Jinsha River Culture, School of Geographic Science and Tourism, Zhaotong University, Yunnan 657000, China. ✉email: libo@bnu.edu.cn

patterns. In the context of global climate change, dam construction and its ecological effects are complex, potential, spatial, cumulative, and unpredictable¹⁸. Quantifying the landscape ecological impact of reservoirs is essential for developing appropriate strategies to reduce adverse impacts on regional environments. Land-use-based landscape ecological security assessments play an important role in the construction of ecological security patterns¹⁹.

For a start, it is necessary to distinguish the fundamental conceptions of land cover and land use. Land cover is generally defined as the coverage of the earth's surface at present that has been formed by natural and anthropogenic influences²⁰; land use is the consequence of long-term interactions between humanity and the natural environment. Land use reflects the utilization manner and condition of the natural properties of land by human beings. In other words, it means according to the natural characteristics of the land and under certain economic and social purposes, humans adopt biological and technological measures to manage and govern land in a long-term and cyclical manner²¹. Landscape refers to the mixture or repetition of regional ecosystem or land use type in a certain area of land²². From the perspective of Geography, it can be seen as geocomplex and land can be used as the landscape types in a sense, landscape-scale was considered as the suitable level to study the environmental impacts from human activities²³. Landscape pattern refers to the spatial structure characteristics of the landscape such as spatial distribution, structure, and configuration of spatial components with a variety of sizes, shapes, and attributes²⁴. It not only shows the heterogeneity of landscape but also reflects the result of natural or human disturbance. These patterns reflect the state of a region's natural environment and influence the stability and order of the ecosystem²⁵. With time, landscape elements are exceptionally resistant to spatial and temporal variability at multiple scales. The gradient effect is evident for different elevations, slopes, and topographic fluctuations²⁶. Topographical factors, including elevation and slope, are among the many factors that are crucial to the natural environment²⁷, which determines the changing direction and ways of landscape types to some extent. Geomorphic conditions are the most critical factor for determining the intensity of human transformations of landscapes. Landscape conditions form landscape evolution patterns that reflect not only the extent of human influence on natural ecosystems but also the responses of human activities triggered by landscape conditions²⁸.

As one of the largest dam reservoirs in the world, the TGR is located in the middle reaches of the Yangtze River²⁹ and is a fragile natural ecosystem^{30,31} with complex and rugged topography that play a big part in the evolution of landscape patterns and intentions of human disruptive activities³². The protection of the ecology and environment in the TGRA plays a crucial role in the green development of the Yangtze River Economic Zone³³. With the construction of the Three Gorges Dam (TGD) and several increases in water levels, many areas upstream of the reservoir have been inundated³⁴. Landscape patterns have also changed greatly with varying degrees of anthropogenic disturbance³⁵. Anthropogenic activities like eco-migrants, urban construction, land use changes, comprehensive supporting facilities, and ecological engineering have resulted in changes in the structure and function of the ecosystem in the reservoir area³⁶. Meanwhile, several measures taken to address agricultural surface pollution and mitigate soil erosion have also led to landscape element changes^{37,38}. Besides, approximately three-quarters of the TGRA is mountainous, and approximately 24.74% of the area is steep and unstable with slopes greater than 25°³⁹. In response to local ecological changes, the Chinese government has actively implemented various large-scale ecological policies and strategies, such as the Forest Projects⁴⁰ and Special Water Management Plan⁴¹. These policies in China in the past directly affected the evolution paths of landscape types and landscape patterns in mountainous areas⁴².

In recent decades, there has been an abundance of national and international research on landscape evolution patterns, as is evidenced by qualitative and quantitative analyses using GIS and RS techniques in conjunction with landscape pattern indices⁴³ that include the relationships between landscape and soil erosion⁴⁴, ecological security patterns⁴⁵, and granularity of landscape pattern effects⁴⁶, among others. As research has progressed, some scholars have introduced landscapes into geography to study the relationship between landscape change and landforms⁴⁷, and the scale of research has gradually shifted from comprehensive evaluations at large scales to in-depth studies at small scales. Moreover, most studies have lacked the dynamics of evaluation results over long periods. At this stage, many researchers have studied the evolution of landscape patterns in the TGRA before and after water storage; and have focused on spatial granularity effects⁴⁸, effects of forest restoration on soil erosion⁴⁹; and cropland patterns and driving forces⁵⁰. Under the contexts of climate change, China's "ecological civilization construction", and economic and social transformation, how did the construction of the TGP affected the landscape element changes in the watershed? What are the differences in landscape evolution characteristics of distinct land types? These are research questions that we try to address.

While past work has mainly focused on landscape change and its evolution characteristics, little information is available on the relationship between landforms (based on elevations and slope gradients) and the evolution of landscape patterns. Landscapes can vary under different landform conditions⁴⁷, and the landform context had a drastic impact on landscape pattern evolution and human disturbance³². The land cover and landscape types in the TGRA have shown great variations due to the influence of water conservancy construction. Therefore, this paper aims to investigate the evolution of each landscape pattern based on elevation and slope zone reclassification in typical watersheds of Chongqing under the context of the TGP construction and operation. The intention is to provide referential significance for land use planning, the establishment of ecological patterns, and environmental protection in the core of the TGRA.

Background: construction timeline of the TGP

In China, the TGP began in 1993 and was completed in 1997 on the upper trunk of the Yangtze River⁵⁰, which is the largest hydroelectric project ever conducted⁵¹, to accommodate flood control, irrigation, increased navigation, and power generation needs^{52,53}. Hydropower construction was completed in 2002³⁹, reservoir filling was initiated in 2003, and impoundment was completed in 2010⁵⁴. By June 2003, the water level was expected to

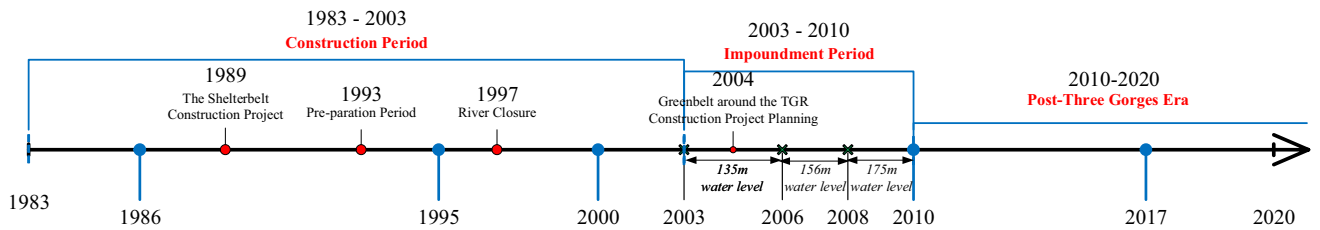


Figure 1. Construction timeline of the TGP.

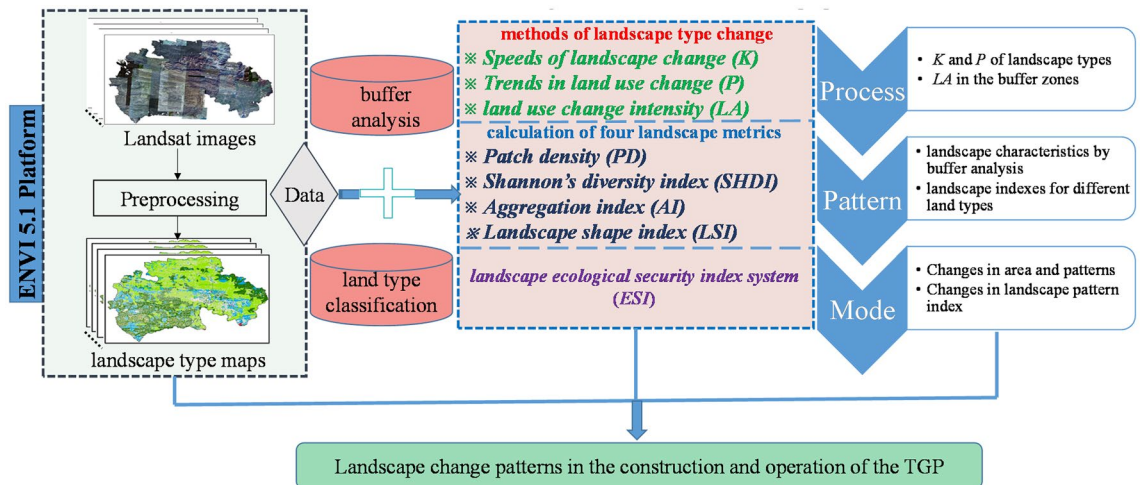


Figure 2. Flowchart for the evolution of landscape change patterns in this study.

increase to 135 m ASL (above sea level), and the first filling stage was completed in 2003⁵⁵. The reservoir level reached 156 m ASL in October 2006. In October 2010, the TGR reached its normal storage level of 175 m ASL for the first time⁵⁶, and approximately 240 km² of citrus and farmland was inundated. Water levels of the TGR are maintained between 145 m ASL from October to March and at 175 m ASL from April to September^{57,58}. By the end of 2010, the TGP had been completed, and the entire reservoir area entered the Post-Three Gorges era³². The formation of the TGRA is a direct consequence of the dam⁵⁹. According to previous relevant studies, the TGRA can be divided into three critical moments: the construction period, impoundment period, and Post-Three Gorges era^{60,61}. Considering the actual situation of the hinterland basin of the reservoir area and the difficulty of data acquisition, this study is divided into three phases: 1986–2000, 2000–2010, and 2010–2017 (Fig. 1).

Materials and methods

The workflow chart for the evolution of landscape change patterns in this study can be summarised as follows (Fig. 2). First, the landscape type maps were classified by ENVI 5.1 platform. Second, based on buffer zone analysis and land type division in ArcGIS 10.2, the methodological evaluation system of this paper is constructed from the methods of landscape element change, calculation of landscape pattern index, and landscape ecological security index. In the results analysis part, we first analyze the *K* (Speeds), *P* (Trends) of landscape types and *LA* (Index of landscape type change intensity) in buffer zones; then the landscape metrics (*PD*, *SHDI*, *AI*, and *LSI*) were computed to reveal the landscape characteristics in buffer zones and land types; finally, combined with the method of landscape ecological security index, we summarize the change modes in area and landscape pattern.

Study area. Tangxi River watershed (TR), Meixi River watershed (MR), and Daning River watershed (DR) in the hinterland of the TGRA were used as case studies (Fig. 3). The study area extends over 31°02'39" ~ 31°44'01" N, 108°37' ~ 110°09'05" E with a total area of 7938 km². It has a northern subtropical humid monsoonal climate, and the prevailing soil types are yellow-brown (Similar to Luvisols in FAO/Unesco) and purple soils (Similar to Regosols in FAO/Unesco)^{62,63}. This area belongs to the Chongqing section of the TGRA, covers four counties (Yunyang, Fengjie, Wushan, and Wuxi) and is the core area for ecological protection and development in northeast Chongqing and is also a fragile and ecologically sensitive area of the TGRA with high mountains and steep slopes¹⁷. The watershed belongs to the first tributary of the north bank of the Yangtze River; TR, MR, and DR are adjacent to each other with various natural social and economic backgrounds. DR is a karst watershed, MR is combined karst and non-karst watershed, and TR is heavily influenced by coal and other industrial wastes with many factories, coal mines, and construction sites. Our study area is representative of the contemporary landscape and is subject to natural and anthropogenic gradients and disturbances.

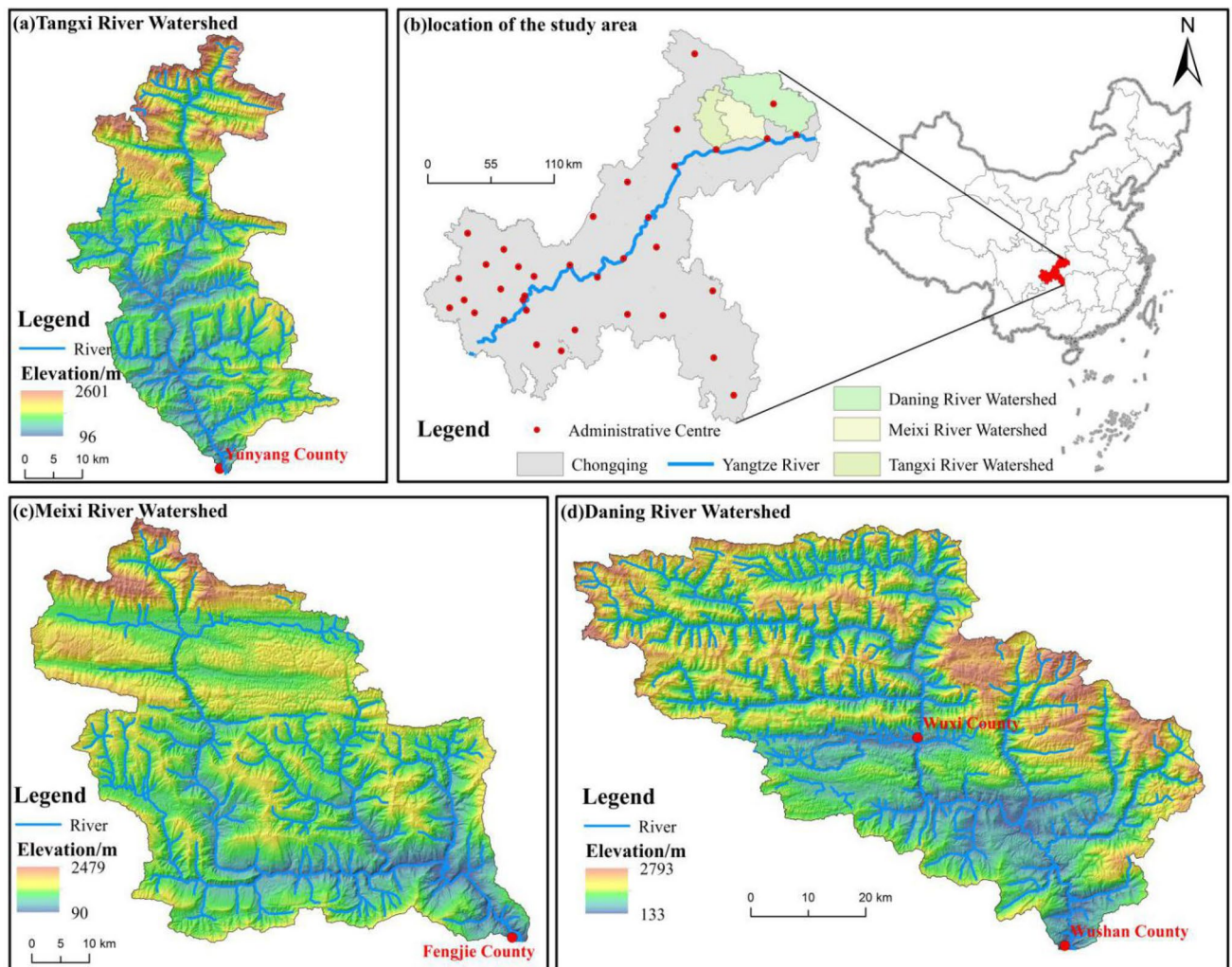


Figure 3. Location and topography of the study area in the TGRA. Maps were generated using ArcGIS 10.2 for Desktop (<http://www.esri.com/software/arcgis>).

Data source and processing. Our basic data sources include multitemporal satellite datasets and a DEM. (1) Landscape type maps for 1986, 2000, 2010, and 2017 (Fig. 4) were obtained from Landsat Thematic Mapper (TM) and Enhanced Thematic Mapper-plus (ETM+) images with 30 m resolution using nonlinear classification and artificial visual interpretation methods. In this paper, the support vector machine method is used in landscape classification and alters manually the misclassified landscapes. By verifying the data accuracy through the confusion matrix and ensuring the Kappa index is above 0.80. The regional landscapes were divided into dry land, paddy field, forestland, shrubland, grassland, water area, built-up areas, and unused land⁶⁴. To meet the needs of the study, land use data from 1986, 2000, and 2010 were rigorously compared with data provided by the “data center for environmental and ecological sciences in western China” of the National Natural Science Foundation of China. For the 2017 land-use data, we strictly compared them with the high-resolution images from resource satellites with a resolution of 2.5 m during the interpretation process. Currently, we are using a combination of random sampling checks and field surveys to ensure data accuracy, and both have an accuracy rate of 92%, which meets the needs of this study. (2) Elevation and slope maps are based on 30 m resolution DEM data, which were downloaded from the CAS Resources and Environmental Science Data Center (<http://www.resdc.cn>). (3) Watershed vector boundaries were extracted from the DEM data with the Hydrology toolset in ArcGIS 10.2.

Results analysis

Changing speeds (K) and trends (P) of landscape types for each land type. We overlaid the landscape type map with the landform classification data by using the Intersection tool in ArcGIS 10.2 software to obtain the landscape types for a variety of land types and then calculated the K and P values based on the methods described in Formula (1) and (2), and the results are shown in Fig. 5.

Figure 5a exhibits the changes in K -values along with landforms for each landscape type. From 1986 to 2000, the K -values of each landform did not change apparently while the area of forestland increased prominently in

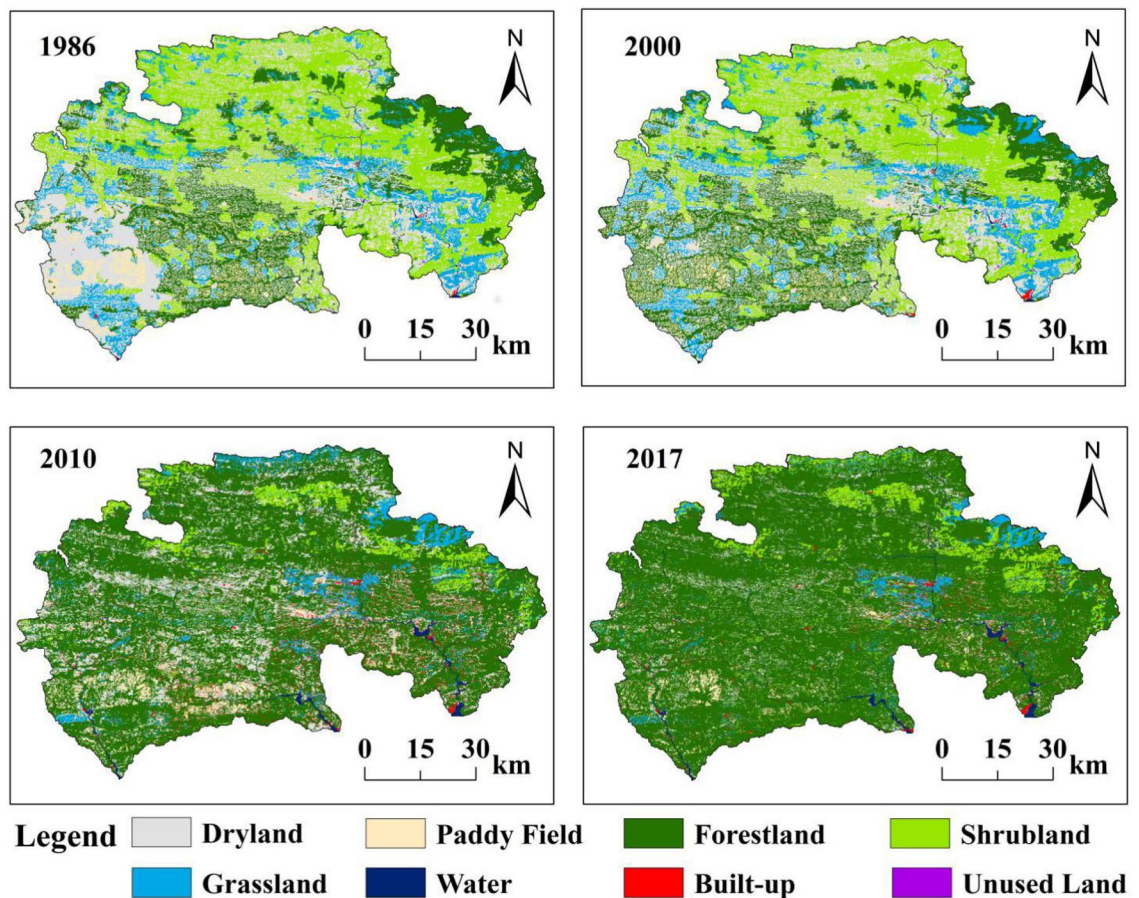


Figure 4. The spatial division of landscape type in the watershed from 1986 to 2017. Maps were generated using ArcGIS 10.2 for Desktop (<http://www.esri.com/software/arcgis>).

valleys with slopes within 15° . From 2000 to 2010, the K -values for altitude and slope changed differently. Waters and built-up areas showed clear increasing trends at elevation gradients below 1000 m, while forestland and waters showed the most pronounced increases in each slope zone. This dramatic increase was mainly due to the rise in reservoir levels and the implementation of the national migration policy. As a result of urbanization, the total amount of built-up areas exhibited an upward trend from 2010 to 2017 in the middle mountainous areas where the elevations were higher than 1500 m.

Figure 5b represents the trend of P in landscape type along with land classification at each time point. In the period 1986–2000, the landscaping trend changed slightly except in valley areas. In this region, forestland, water, and built-up areas all expanded in an “upward” fashion. From 2000 to 2010, land use trends varied for elevation and slope. Cultivated land increased for slopes less than 8° ; in areas below 1000 m elevation and with slopes less than 15° , settlements were the dominant landscape, and in both low and steep slope areas, water sources increased greatly as the water level rose. From 2010 to 2017, the landscape trends changed slightly, except in the valley and mid-mountain areas. In the valley areas, shrublands expanded in an “ascending” fashion. For the mid-hills, the built-up area expanded remarkably in an “ascending” state.

In general, landscape types in the watershed change at different rates and trends along elevation, slopes, and buffers, and the changes are phased and exhibit a process that changes from quantitative to qualitative. The period from 2000–2010 experienced the most intense landscape evolution during the impoundment period.

Analysis of changes in the level of land use degree (LA) in the buffer zones. We used the Intersect tool in ArcGIS 10.2 software to overlay the landscape types of different landform maps with the watershed buffers and then calculated the index of landscape type change intensity (LA) values based on the method described in Formula (3), and the results are shown in Figs. 6 and 7.

Variations in buffer distance reflect some extent the variations in upstream and downstream distances. Figure 6 shows that the LA of each buffer zone in the basin showed a general downward trend that reached a maximum value for a buffer zone of 30 km and a minimum value for a buffer zone of 110 km. Within the 30 km buffer zone, the terrain is relatively flat, dominated by micro-slopes, and influenced by the intensity of human activities, while the degree of development is relatively high.

As illustrated in Fig. 7, the landscape changes in different land types in buffer zones of the watersheds varied from 1986 to 2017. Within the 30 km buffer, all land types in the TR had the highest landscape synthesis with reduced fluctuations around them, while the landscape synthesis in the MR and DR buffers showed notably

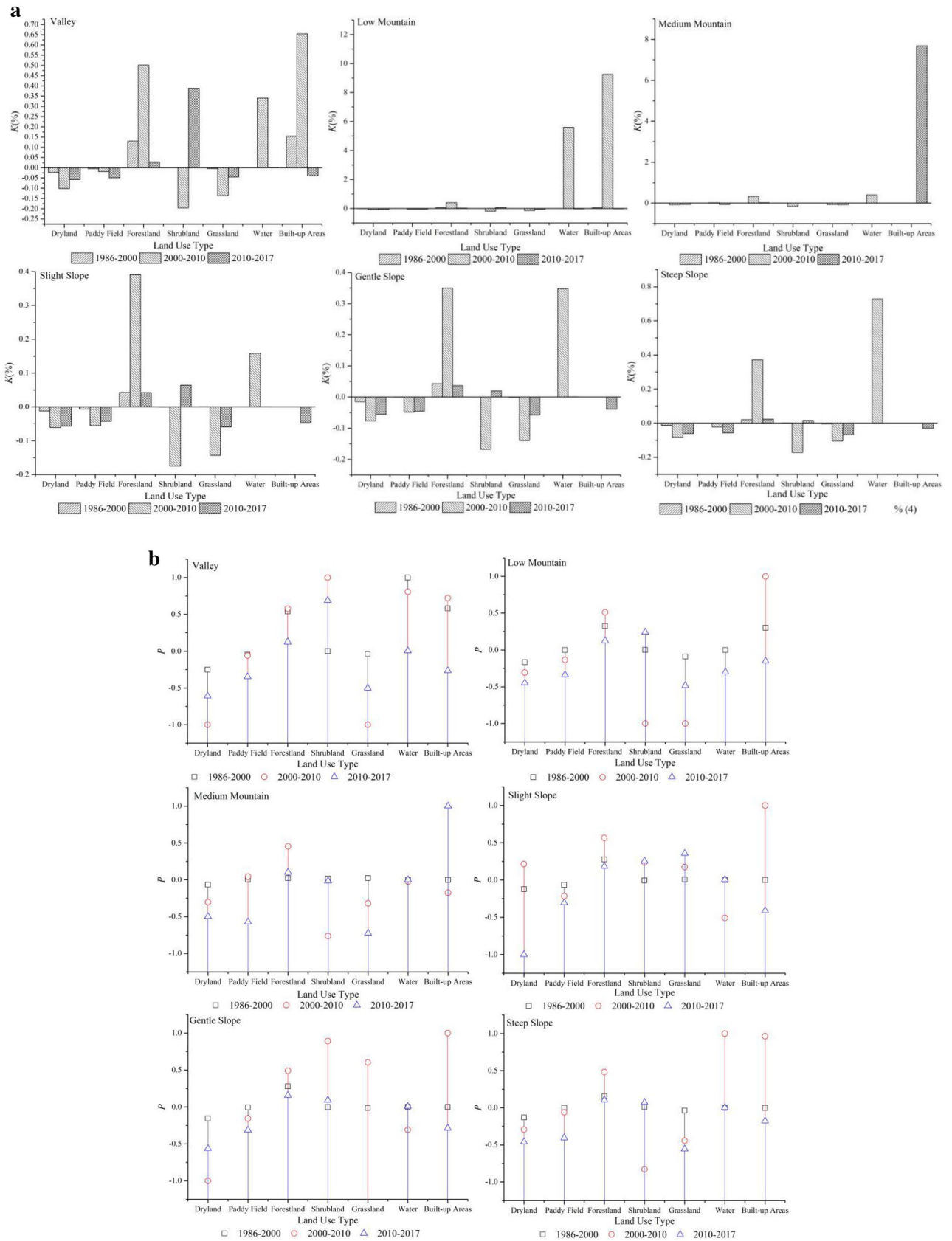


Figure 5. (a) Speed of different land cover for different landforms of the watersheds, (b) The trend of different landscape types for different landforms of the watershed.

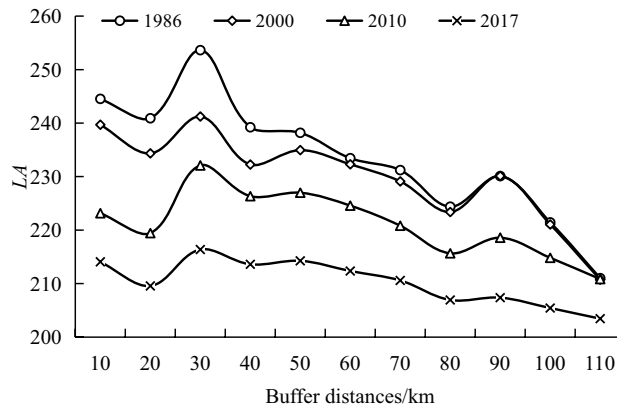


Figure 6. Comprehensive landscape degree index in the buffer zone of the watershed.

different features across the different media. For the MR, the largest number occurred for a buffer zone of 10 km during the period of 1986–2000 among each geomorphic type. The 50 km buffer zone was largest in 2010 for the valley, medium-mountain, and steep slope areas, while the 80 km buffer zone was largest for the low-mountain, slight slope, and gentle slope areas. Unlike 2010, the *LA* of the MR showed an “N” type trend in elevation with the increase of buffer distance, and a “W” type trend in slope. This illustrates that the spatial distribution of the *LA* in the MR showed an obvious spatial heterogeneity in terms of elevation and slope. In 2017, except for the gentle slope, the 70 km buffer zone was the largest, while the other geomorphic areas were all largest in the 10 km buffer zone. The maximum value of the *LA* among the geomorphic areas in the DR occurred in different buffer zones. By comparing relevant research results, it was found that the 30 km buffer zone in the TR, 50 km buffer zone in MR, and 10 km buffer zone in the DR were mainly 800–1000 m ASL, and the lithology was mainly sandstone and mud shale, which are easily reclaimed for farmland. Human activities were relatively concentrated⁶⁵, so *LA* was relatively high.

Four landscape indexes (*PD*, *AI*, *LSI*, *SHDI*) characteristics by buffer analysis. We overlaid the landscape type map with the buffer data using the Intersect tool in ArcGIS 10.2 software to obtain landscape types with different buffers and then calculated *PD*, *SHDI*, *AI*, and *LSI* values on the FRAGSTATS 4.2.1 platform; and the results are shown in Fig. 8.

Figure 8 shows that *PD* and *AI* both increased at four-time points, while *SHDI* and *LSI* decreased. In particular, from 1986 to 2000, the *PD* values in all three watersheds were less than 2, and these small values were less affected by the construction of the TGP. After 2000, due to the implementation of ecological migration and circular economic development, there was an obvious increase in *PD* values and decrease markedly in *SHDI* and *LSI* values. With increasing buffer distances, *PD* showed an appreciable upward trend in MR and DR and increased volatility in TR. During the study period, *SHDI* showed a decreasing trend as the buffer distance increased. This indicates the transition from a diverse landscape of cultivated land, forest, shrub, and grass to a single landscape dominated by forestland in the watershed with the advent of the Post-Three-Gorges Era. For *AI* values over 90, landscape aggregation is evident. With increasing buffer distance, the *LSI* showed an inverted U trend. In 2017, the *AI* and *PD* in the DR show the lowest value in 80 km buffer zones, this indicates the highest degree of landscape fragmentation in this zone.

Overall, the landscape pattern characteristics in the watershed showed a noticeable change as a result of TGP progression, with an upward trend in *PD* and the downward trend in *SHDI*, *AI*, and *LSI*. This may imply an increase in ecosystem quiescence.

Characteristics of landscape indexes (*PD*, *AI*, *LSI*, *SHDI*) for different land types. The different trends of the different landscape indices are shown to be under the influence of major water projects and rapid urbanization (Fig. 9). From 1986 to 2017, there was a distinct increase in the *PD* index, a wave-like downward change in the *SHDI* and *LSI* indices, and a less pronounced change in the *AI*. These changes indicate that the fragmentation degree increased, the landscape multiplicity decreased, and the landscape shape was relatively normal with the progression of the TGP. The landscape indices of different landform were obvious distinctions.

Specifically, *PD* tended to increase with elevation and decrease with slope along with greater fragmentation of valleys and steep slopes; *SHDI* decreased with elevation and slope, and the ecosystem may be more homogeneous; *AI* decreased first and then increased with elevation and slope, respectively, with greater aggregation of elevation than slope; *LSI* increased first and then decreased with elevation and slope while showing “N”-shaped changes. The landscape patterns were more complex and irregular in low mountains and gentle slopes.

Characteristics of changes in landscape types and landscape indicators before and after the impounding period. *Changes in area and patterns of landscape types over three time periods.* From the mid-1990s to the present, the landscape of the TGRA has undergone dramatic changes due to the construction of the Three Gorges Hydropower Station (TGHS), which has attracted much attention³⁸. Due to intense and

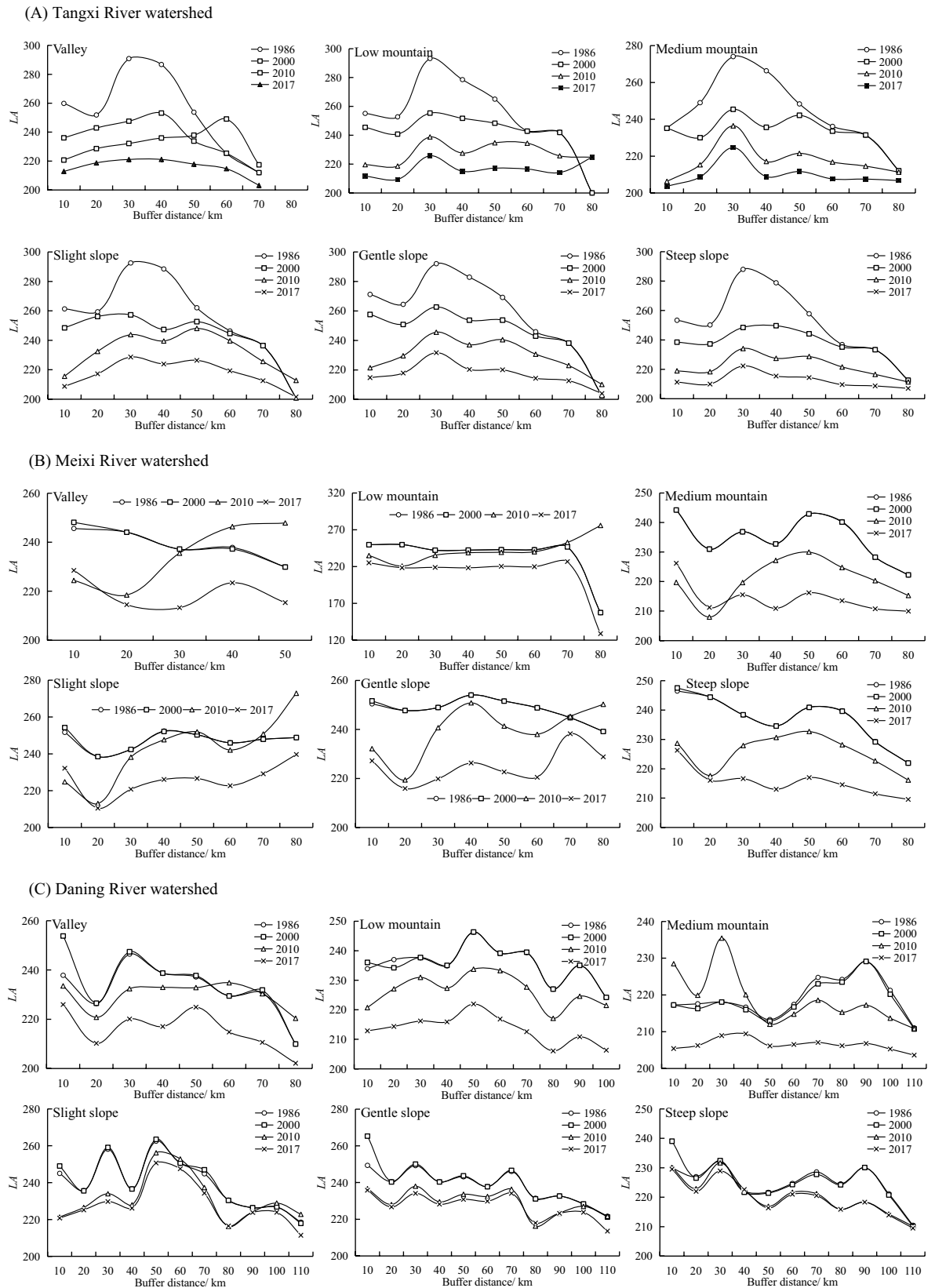


Figure 7. Comparison of LA in different buffer zones of watersheds from 1986 to 2017.

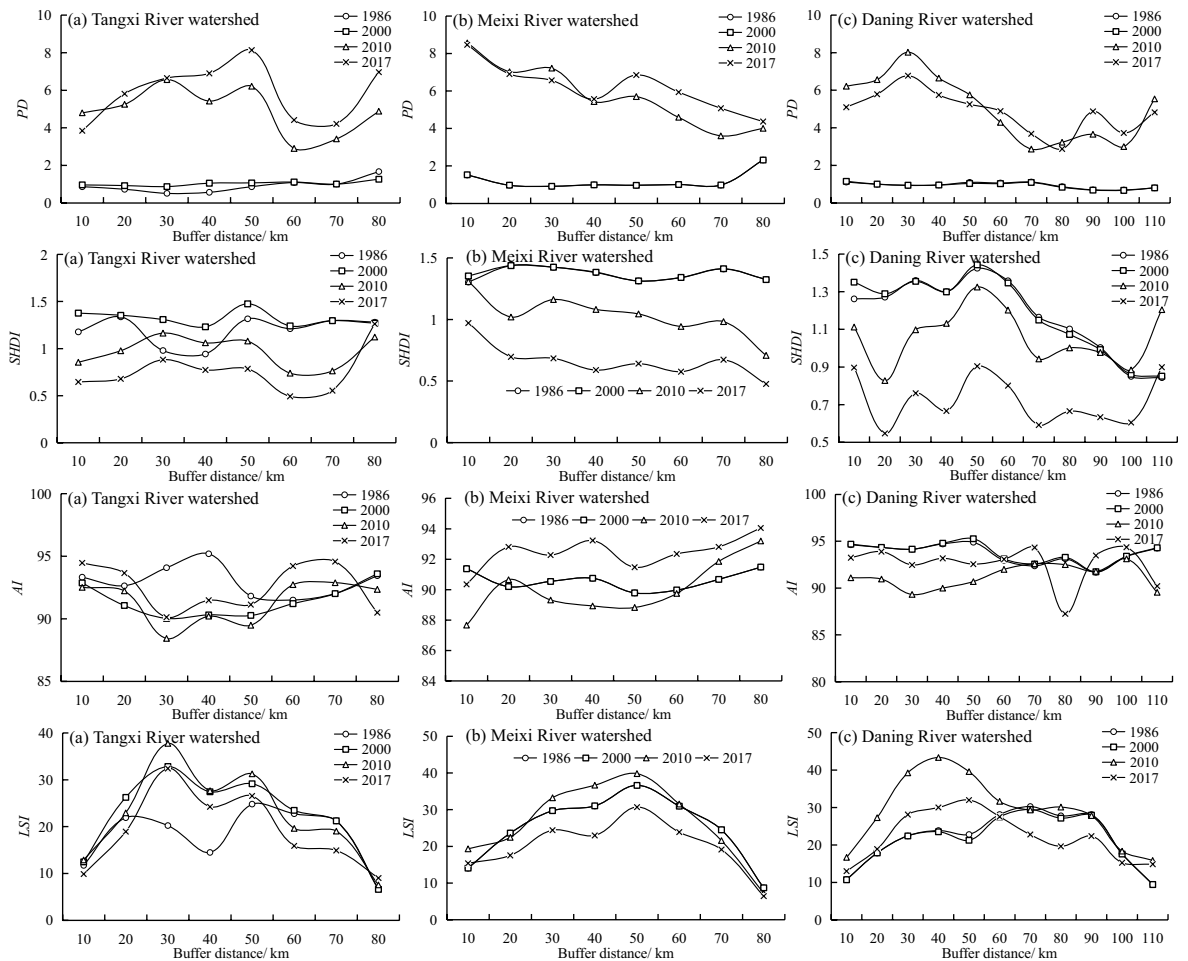


Figure 8. Changes in landscape metrics along with the buffer distance of the watershed from 1986 to 2017.

complex human pressures, the landscape structures and ecosystem service functions in the region have experienced frequent changes over the last 30 years. A large amount of land has been flooded due to the construction of hydroelectric dams and infrastructure. The relocation of immigrants and redevelopment of towns and cities have led to a dramatic decrease in the area of water in cultivated land and experienced a deceleration in growth, which is very consistent with the results indicated by the previous studies³⁰. The conversion of cropland to forest has been the dominant landscape transformation process⁴⁹, the area of cropland around the TGRA is decreasing³⁰, and approximately 28% of farmland in China's mountainous counties is abandoned⁶⁶. Landscape change is phased⁶⁷, and long-term stable landscape transitions can be used to reveal models of landscape evolution (Fig. 10).

In the first period (before 2000), there were conspicuous inter-conversions between different landscape types³⁹ with concentrated and contiguous agricultural land forming the main landscape type of the watershed. The composite index of landscape extent was higher than in the other two periods, and the trend of landscape ecological security was improving.

The direct impact on the watershed during the impoundment period from 2000 to 2010 refers to the conversion of cultivated land to water bodies⁶⁸. During this period, landscape changes manifested as an increase in forestland due to the implementation of natural reserves and government forest projects. Arable lands with slopes greater than 25° were best converted to the forest in accordance with the arable land conversion policy⁴⁰. At the same time, due to land abandonment, arable land was converted to grassland or other landscape types. The general trend of landscape change was from low-cover types to high-cover types. The overall ecological security situation has declined due to the equal emphases on development and conservation.

At the present stage (after 2010), forests form the main landscape type of the watershed. As a result of China's policies of "ecological civilization construction" and targeted poverty alleviation, farmers earn income by transforming their agricultural production methods to achieve unity of economic and ecological benefits⁶⁹. The ecological security situation of the landscape shows a favorable development trend.

The landscape is affected by complex topographic variables such as elevation and slope. Kelarestaghi⁷⁰ found that altitude and slope are the physically effective factors that drive landscape change. Given previous work, we hypothesized that the watershed contained five patterns of landscape evolution with increasing elevation, slope, and buffer zone width under the influence of the TGP from 1986 to 2017 (Fig. 11). During the first period from 1986 to 2000, patterns A, B, C, and E occurred in valleys with slopes less than 15°, all buffer zones with altitudes

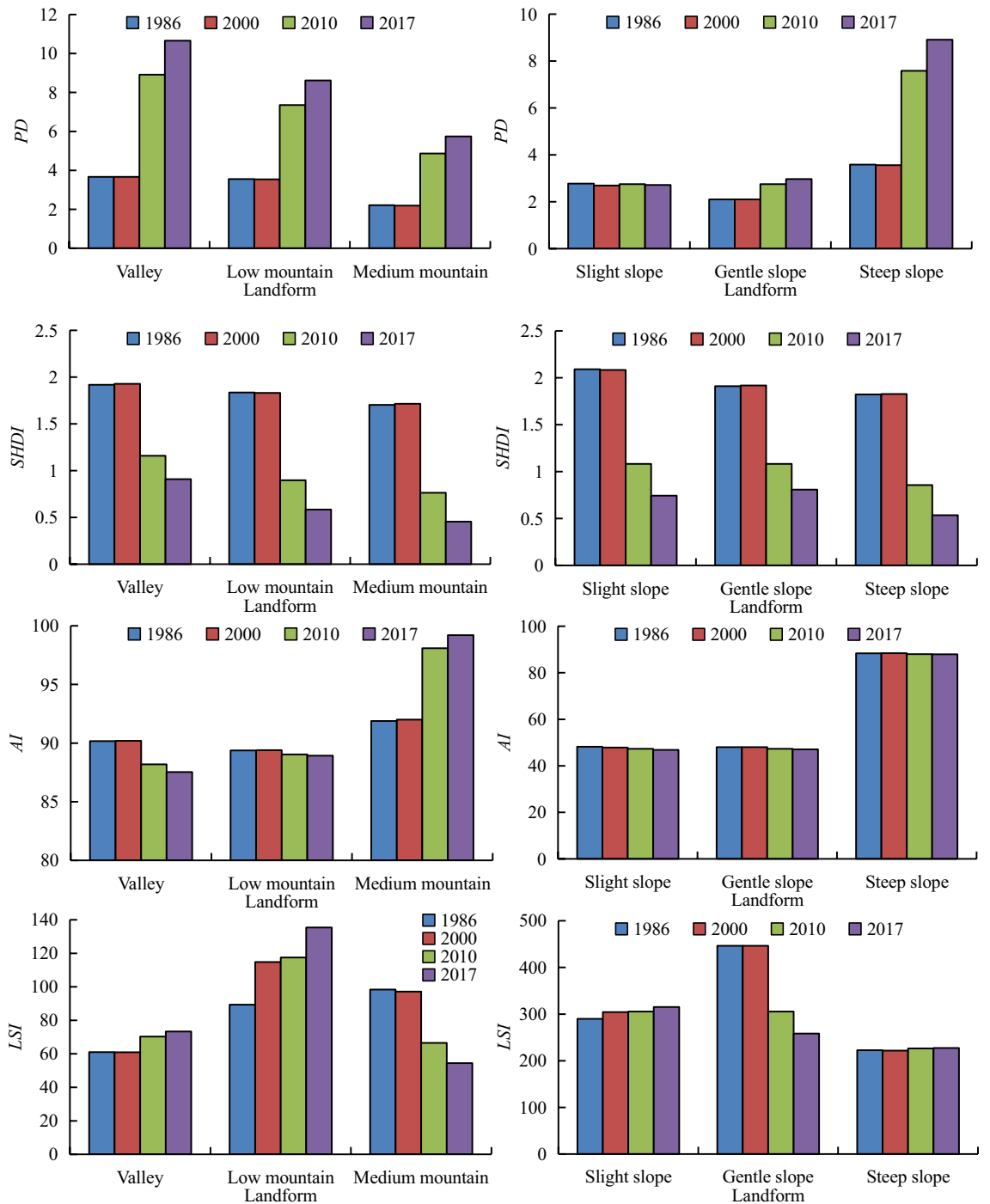


Figure 9. Changes in landscape index along with landforms from 1986 to 2017 in the watershed.

less than 500 m, and slopes less than 8°. From 2000 to 2010, the landscape patterns of all spatial regions, especially those regions with slopes less than 15° and altitudes less than 1,000 m, were deeply influenced by human activities, and the main patterns were Mode A and Mode C. Unlike the previous phase, Mode A was distributed in the slight slope belts within the 50 km buffer zone due to relocation and urban renewal. From 2010 to 2017, the landscape of the whole spatial region for Modes A, C, and E was especially located in areas with slopes less than 8° and elevations less than 500 m. Model B was distributed within a 40 km buffer zone with slopes less than 15° and elevations greater than 1,000 m.

Changes in landscape pattern index over three time periods. Landscape types exhibited a distinct transformation phase before and after impoundment and are sensitive to elevation and slope³⁹. In this context, the changes in the landscape pattern index in this study were divided into three periods during the construction of the TGR, just as shown in Fig. 12. In the first stage (before 2000), the landscape pattern index change was not obvious, the

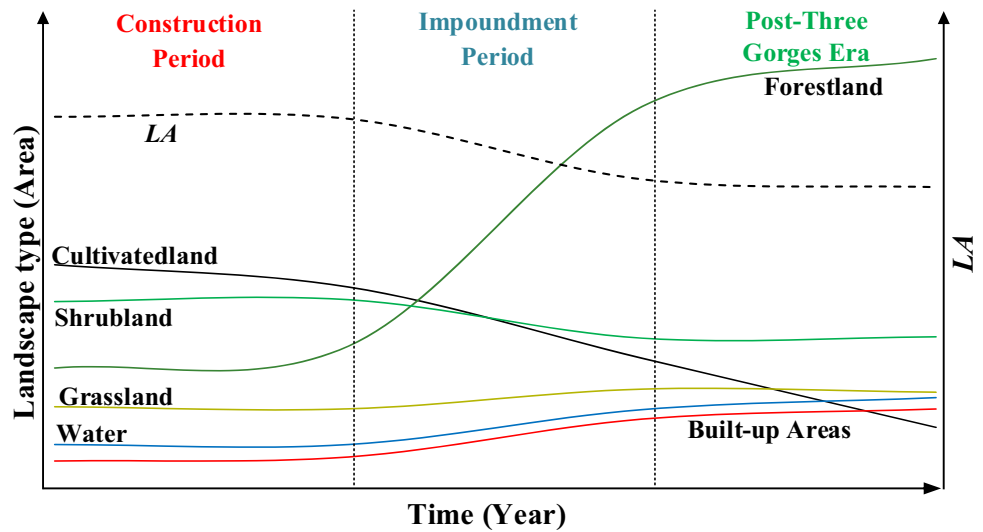


Figure 10. Change of landscape types in the watershed.

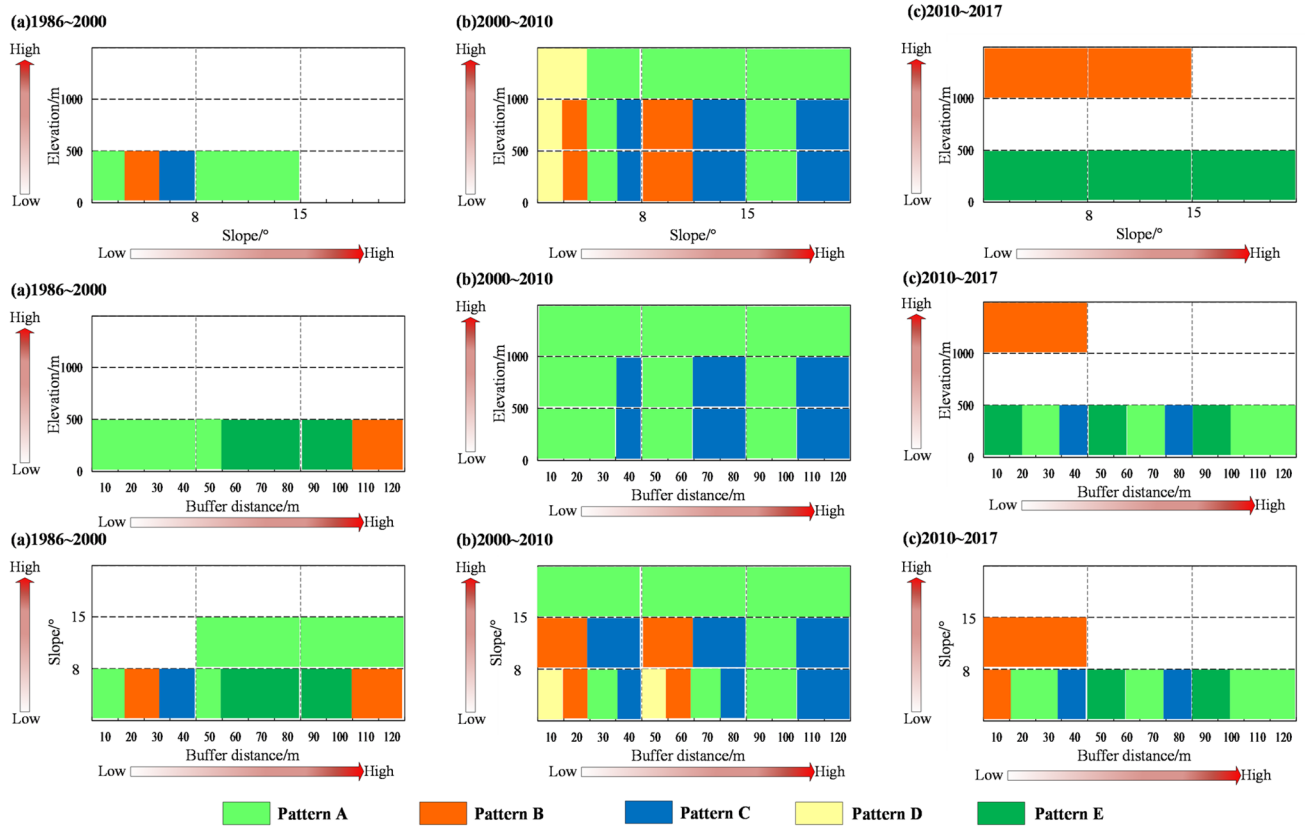


Figure 11. Landscape evolution model in a typical watershed of the TGRA. Pattern A: conversion of other landscape types to forestland; Pattern B: conversion of other landscape types to built-up areas; Pattern C: conversion of other landscape types to water bodies; Pattern D: conversion of other landscape types to farmland; Pattern E: conversion of other landscape types to shrubland.

transition of landscape categories was stable, and the landscape pattern was reflected by the reclamation of agricultural land, which increased rapidly³⁵. In the impoundment period from 2000 to 2010, the *PD* index exhibited a remarkable increasing trend, *SHDI* showed a decreasing trend, and the changes in the *AI* and *LSI* indices were not obvious. For the cases of economic development and ecological protection, a landscape pattern with high heterogeneity and low diversity was present, with an increase in forest and water area being the most notable

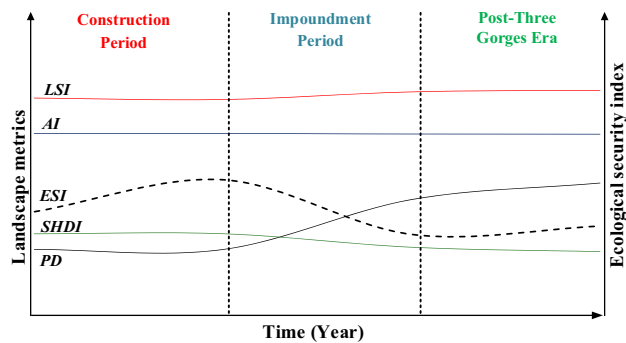


Figure 12. Change in landscape pattern indexes in the watershed.

landscape dynamic pattern. In recent decades, (after 2010), the *PD* index has dramatically increased, the *SHDI*, *AI* and *LSI* indices have not changed notably, and the landscape has shifted from diversified to relatively unitary.

From 1986 to 2017, the *ESI* showed a trend of *N*, which indicated that the spatial structure of the landscape was more stable and ecological security was more reasonable due to the implementation of policies such as the return of farmland to forest and designation of red lines for ecological protection. Due to the disturbing effects of the water conservancy construction itself, it was more difficult to restore the ecosystem to its preconstruction state. As the most basic and important type of landscape, both the natural environment and human activities can tremendously trigger landscape differences. The study of landscapes and their mechanistic driving factors are conducive to the optimization and improvement of policy mechanisms.

The changes in landscape types and landscape pattern indices at different stages are consistent with the laws and needs of reservoir construction. Over time, the spatial structure of the landscape becomes more stable and ecologically safe.

Discussion and Conclusion

Discussion. Over the 1986–2017 period, the arable landscape area of watershed decreased in each landform, which is in agreement with the findings of MEE (2018)⁷¹. We have shown that the landscape in the watershed changed from arable land to forestland, and Xu et al. (2020)⁷² found that cropland area in the TGRA has dropped from 29.0% in 1997 to 22.9% in 2016. Our finding supports the contention that ecological functions have been improved (SAGCAE, 2010)⁷³, however, landscape ecological security can hardly revert to that before dam construction. Our study considered topographical factors are the foundation of landscape pattern formation and their spatial characteristics influence the evolution process of the landscape. Based on the elevation and slope characteristics, we divided the whole watershed into six categories and presented the landscape change pattern at each land type. In addition, we analyzed the differences of *LA* and landscape indexes of each land type for three different periods with the increase of buffer distance.

There are some limitations in our study that deserve mention. Firstly, it is difficult to precisely quantify modes of landscape change patterns in watersheds. Secondly, due to the complexity of the data acquisition on socioeconomic aspects of the watershed, this paper failed to reveal the driving mechanisms of the evolution of landscape patterns in the watershed. Lastly, we did not consider the watershed in the head and tail of the TGRA due to the lack of monitoring data.

Conclusion. In the context of China’s “ecological civilization construction”, considering the noticeable impact of multiple stressors of TGP construction on ecological changes, this paper analyzes the changes in the degree of landscape evolution through measures related to the analysis of landscape type changes and landscape patterns in typical watersheds of the TGRA from 1986–2017 and draws the following conclusions.

Changes in the landscape patterns of the watershed are closely related to the construction of the TGP. During the construction period from 1986–2000, landscape types and landscape patterns change insignificantly, with arable land being the dominant landscape transformation process. From 2000 to 2010 (i.e., impoundment period), land use showed dramatic changes, with the conversion of arable land to forestland being the dominant landscape transformation process, water area changes were not obvious, and landscape types showed different trends in different regions. The results indicate that ecological conservation policies have a greater impact on landscape type change than reservoir impoundment. After 2010, landscape types changed more in areas with elevations below 500 m and slopes below 8°. Changes in land use type in the watershed brought landscape changes, and landscape fragmentation and diversity showed increasing trends throughout the study period.

With the increase of buffer distance, *LA*, *PD*, *SHDI*, *AI*, and *LSI* show negligible differences within different land types. *LA* of each buffer zone in the basin showed a general downward trend that reached a maximum value for a buffer zone of 30 km and a minimum value for a buffer zone of 110 km. Due to the complexity and diversity of the geographic environment in three watersheds, the distribution of *LA* has obvious spatial heterogeneity. As for the four landscape indexes, the landscape pattern characteristics in the watershed evidently changed as a result of TGP progression, with an upward trend in *PD* and the downward trend in *SHDI*, *AI*, and *LSI*. From 1986 to 2017, the *ESI* showed a trend of *N*, which indicated that the spatial structure of the landscape was more

Elevation zone/m	Geomorphologic classification	Area percentage	Slope zone/°	Slope classification	Area percentage
< 500	Valley	11.32	< 8	Slight slope	3.72
500–1000	Low Mountain	37.15	8–15	Gentle slope	8.76
> 1000	Medium Mountain	51.53	> 15	Steep slope	87.52

Table 1. Elevations, slope reclassifications, and land type classifications and their area percentages (%).

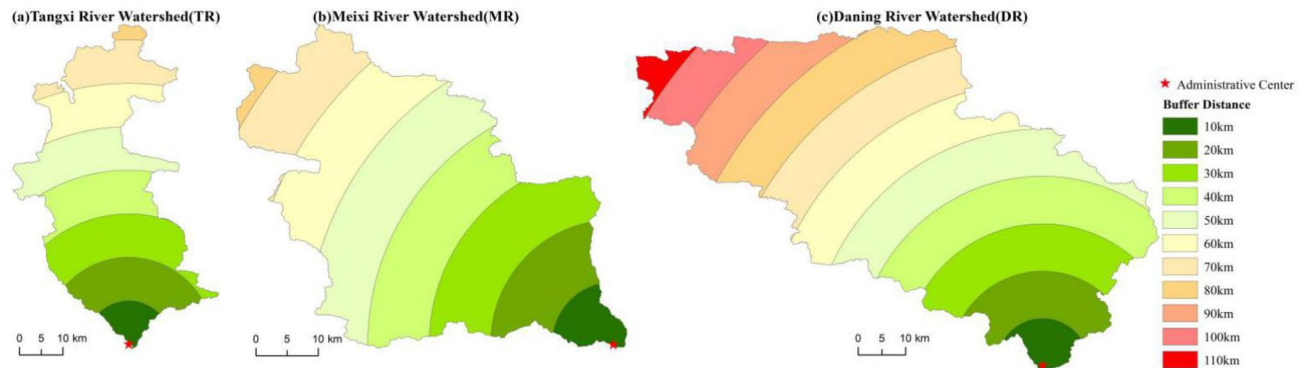


Figure 13. Setting up of watershed buffer zone. Maps were generated using ArcGIS 10.2 for Desktop (<http://www.esri.com/software/arcgis>).

stable and ecological security was more reasonable due to the implementation of policies such as the return of farmland to forest and designation of red lines for ecological protection.

In this study, we employed GIS and RS tools, buffer analysis, and calculations of K , P , LA , and landscape pattern indices to analyze the spatial–temporal differential characteristics of the regional landscapes that were induced by dam construction and reservoir impoundment. In view of the phase of the large water conservancy project and the particular properties of the watershed and combined with the classification of land types based on elevation and slope gradient, our study reveals the landscape ecological effects over the long term sequenced from the perspectives of speed, tendency, intensity, and landscape pattern. Reservoir construction is an important human activity, and relevant studies of landscape models and patterns before/after reservoir construction can help us understand the generalizations of regional sustainable development. The landscape pattern in the riparian zone of the Three Gorges Reservoir and its response to ecological safety will be studied in the future.

Methods

Elevation, slope reclassification, and land types classification. Watershed elevations were reclassified into < 500 m, 500–1000 m, and > 1000 m based on geomorphological classification criteria using 30 m spatial resolution DEM data. Slope (degrees) was extracted from the DEM. Using the Slope Spatial Analysis tool in the ArcGIS software, we obtained a rasterized slope map of the study area. The slopes were reclassified into three grades of < 8°, 8° ~ 15° and > 15°^{74,75}. Based on the elevation and slope characteristics, the land types were divided into six main categories, with watershed classifications and their area percentages shown in Table 1. Watersheds are mountainous and are present where more than 87% of the area has a topographic slope of more than 15°.

Landscape spatial analysis: buffer analysis. As the basic contents of GIS spatial analysis, buffer analysis is the effective vehicle to describe the impact of geographical objects on their surroundings and to solve the problem of spatial proximity⁷⁶. It is to create a faceted area around the analysis object at a certain distance to identify the radiation or influence of the analysis object on neighboring objects. To reflect the changes in landscape types and landscape metrics at different distances from the mainstream of the Yangtze River, this study analyzed a buffer zone with a radius of 10 km, which was centered on the outlets of the lower reaches (county government locations) of the three watersheds, to create a buffer zone, as shown in Fig. 13. The generated buffer zone was used to segment the landscape type status map to obtain landscape type maps of different buffer zones for each period. The land-use change velocity index (K), land-use change trend (P), and land use degree index (LA) were calculated by overlay analysis to analyze land use changes in different elevations and slope zones. This paper then explores the patterns of land use evolution in different buffer zones over different periods in the watershed.

Data analysis methods of landscape type change. *Speeds of landscape change (K).* The single land use dynamic degree (K) is used to reflect the rate of change for a certain landscape type and the differences between each type^{38,55,77}, the mathematical expression is as follows:

Item	Abbr	Ecological significance	Mathematical expression	Data range
Patch density	<i>PD</i>	Landscape fragmentation	$PD = N/A$	$PD > 0$
Shannon's diversity index	<i>SHDI</i>	Balanced and heterogeneous distribution of different patch types within the region	$SHDI = -\sum_{i=1}^n P_i \ln P_i$	$SHDI \geq 0$, without limit
Aggregation index	<i>AI</i>	Dispersion degree among the same landscape type	$AI = \left[\sum_{i=1}^m \left(\frac{g_{ij}}{\max \rightarrow g_{ij}} \right) \right] (100)$	$0 \leq AI \leq 100$
Landscape shape index	<i>LSI</i>	Plaques complexity	$LSI = \frac{0.25E}{\sqrt{A}}$	$LSI \geq 0$, without limit

Table 2. Selected landscape metrics and their ecological significance. *A* is the total landscape area; P_i is the area proportion of landscape *i*; g_{ij} is the number of similar adjacent patches of plaque-type; *E* is the total length of all patch boundaries in the landscape.

$$K = \frac{U_{t2} - U_{t1}}{U_{t1}} \times \frac{1}{t2 - t1} \times 100\% \quad (1)$$

where U_{t1} is the area of a land use type at time $t1$ and U_{t2} is the area of the land use type at time $t2$; if t is set as one year, the value K is the annual comprehensive change rate of land use in the watershed.

Trends in land use change (*P*). In our study, a single land use spatial change trend model was used to reflect the changing trend of landscape types⁷⁸. The basic equation is shown below:

$$P = \frac{U_{t2} - U_{t1}}{\Delta U_{out} + \Delta U_{in}} \quad (2)$$

where P denotes the change trend index of different land use types in the river watershed; ΔU_{out} represents the sum of the areas converted from a certain land use type to other land use types during the research period; ΔU_{in} is the sum of the areas of other land use types that were converted into this type during the research period; when $-1 < P \leq 0$ the scale of the land use type has decreased and is in a “weak” state and when $0 < P \leq 1$ the scale of the land use type has expanded and is in a “rising” state.

Calculation of the index of landscape type change intensity (*LA*). The synthetic landscape dynamic attitude index is used to characterize the breadth and depth of the landscape⁷⁹. According to the actual classification of land use types, they were divided into specific sets at four levels: I for unused land; II for water, bush, forestland, grassland; III for paddy field, dry land; and IV for built-up land. This division is represented by the following equation:

$$LA = 100 \times \sum_{i=1}^n A_i \times C_i \quad (3)$$

where LA denotes the synthetic land use dynamic degree and varies from 100 to 400, A_i is the grade index of grade i , C_i represents the grade i land area percentage for the entire region, and n is the number of grades, e.g., $i = 1, 2, 3, 4$.

Selection and calculation of four landscape metrics. Landscape index is a quantitative research metric used to characterize landscape pattern features and process changes, and to establish associations between patterns and landscape processes. The landscape-level index reflects the overall structural characteristics of the landscape. Here, according to the implications and usefulness of various landscape indices^{80,81}, four landscape indices, namely, patch density (PD), Shannon's diversity index ($SHDI$), aggregation index (AI), and landscape shape index (LSI) were selected and measured by using FRAGSTATS 4.2 software⁸² to characterize the general landscape, and the information for the selected landscape is shown in Table 2. Where, PD reflects the complexity of landscape spatial structure and, to some extent, the level of landscape disturbance by human activities; $SHDI$ reveals landscape heterogeneity characteristics, and $SHDI$ values increase with the increase of landscape patch types and the equalization of its area weight; AI describes the aggregation degree among landscapes and reflects the dispersion degree among the same landscape type; LSI represents the index of patch shape complexity, the larger the LSI index, the more complex the patch shape.

Establishment of a landscape ecological security index system. The landscape ecological security index reflects the impact of natural and human pressures on ecological security from the landscape perspective. In this study, however, the landscape disturbance index (LDI) and landscape vulnerability index (LVI) was calculated as causal indices to measure landscape ecology based on representative landscape indices^{83,84}. In general, the greater the level of disturbance and vulnerability, the lower the level of ecological safety. The landscape disturbance index (LDI) is generally reflected by the combined state of patch density (PD), fractal dimension ($FRAC$), and Shannon's diversity index ($SHDI$). The LDI is calculated by the following formula.

$$LDI = \alpha PD + \beta SHDI + \gamma FRAC \quad (4)$$

where the index weights are α , β , and γ , respectively, and they are given values of 0.5, 0.3, and 0.2.

In general, landscape ecological security is related to landscape vulnerability, and the landscape vulnerability index (*LVI*) mainly reflects the degree of variation of each landscape type in the watershed after being disturbed. In turn, there are differences in the degree of disturbance resistance and sensitivity of different landscape types. We assigned vulnerability values to different landscape types: built-up areas 1, forestland and shrubland 2, grassland 3, cultivated land (dryland and paddy field) 4, and water area 4.

Thus, it is possible to construct a landscape ecological security index (*LESI*) based on normalized landscape metrics, which are area-weighted and summed by *LDI* and *LVI* combined. *LESI* is represented by the following equation.

$$LESI_k = \sum_{i=1}^n \frac{A_{ki}}{A_k} \times (1 - 10 \times LDI_i \times LVI_i) \quad (5)$$

where $LESI_k$ is the landscape ecological security index of the evaluation unit k , n is the number of evaluation units, A_{ki} is the area of landscape type i in the evaluation unit k , and A_k is the total area of the evaluation unit k .

Received: 20 November 2020; Accepted: 31 March 2021

Published online: 29 April 2021

References

1. ICOLD (International Commission On Large Dams). World Register of Dams. Preprint at https://www.icold-cigb.org/GB/world_register/world_register_of_dams.asp (2020).
2. Lehner, B. *et al.* High resolution mapping of the world's reservoirs and dams for sustainable river flow management. *Front. Ecol. Environ.* **9**(9), 494–502. <https://doi.org/10.1890/100125> (2013).
3. Moussa, A., Soliman, M. & Aziz, M. Environmental evaluation for High Aswan Dam since its construction until present. In: Sixth International Water Technology Conference, IWTC, Alexandria, Egypt (2001).
4. Strand, H., *et al.* Sourcebook on remote sensing and biodiversity indicators. NASA-NGO Biodiversity Working Group and UNEP-WCMC (2007).
5. Grumbine, R. E. & Pandit, M. K. Threats from India's Himalaya dams. *Science* **339**(6115), 36–37. <https://doi.org/10.1126/science.1227211> (2013).
6. Chen, C., Ma, M., Wu, S., Jia, J. & Wang, Y. Complex effects of landscape, habitat and reservoir operation on riparian vegetation across multiple scales in a human-dominated landscape. *Ecol. Indic.* **94**, 482–490. <https://doi.org/10.1016/j.ecolind.2018.04.040> (2018).
7. Milliman, J. D. & Meade, R. H. World-wide delivery of river sediment to the oceans. *J. Geol.* **91**, 1–21 (1983).
8. Tonkin, J. D. *et al.* Flow regime alternation degrades ecological networks in riparian ecosystems. *Nat. Ecol. Evol.* **2**, 86–93. <https://doi.org/10.1038/s41559-017-0379-0> (2018).
9. Nillson, C., Reidy, C. A., Dynesius, M. & Revenga, C. Fragmentation and flow regulation of the world's large river systems. *Science* **308**, 405–408 (2005).
10. Mitsch, W. *et al.* Optimizing ecosystem services in China. *Science* **322**(5901), 528 (2008).
11. Stone, R. Three Gorges Dam: into the unknown. *Science* **333**, 817 (2008).
12. Fu, B. J. *et al.* Three Gorges Project: efforts and challenges for the environment. *Prog. Phys. Geogr.* **34**(6), 741–754. <https://doi.org/10.1177/0309133310370286> (2010).
13. Xu, X. B. *et al.* Unravelling the effects of large-scale ecological programs on ecological rehabilitation of China's Three Gorges Dam. *J. Clean Prod.* <https://doi.org/10.1016/j.jclepro.2020.120446> (2020).
14. Yaeger, M. A., Massey, J. H., Reba, M. L. & Adviento-Borbe, M. A. A. Trends in the construction of on-farm irrigation reservoirs in response to aquifer decline in eastern Arkansas: implications for conjunctive water resource management. *Agric. Water Manage.* **208**, 373–383. <https://doi.org/10.1016/j.agwat.2018.06.040> (2018).
15. Bai, J. *et al.* Soil organic carbon contents of two natural inland saline-alkalined wetlands in northeastern China. *J. Soil. Water Conserv.* **62**(6), 447–452 (2007).
16. Chen, L. G., Qian, X. & Shi, Y. Critical area identification of potential soil loss in a typical watershed of the Three Gorges Reservoir Region. *Water Resour. Manag.* **25**(13), 3445–3463. <https://doi.org/10.1007/s11269-011-9864-4> (2011).
17. Xiao, Q., Xiao, Y. & Tan, H. Changes to soil conservation in the Three Gorges Reservoir Area between 1982 to 2015. *Environ. Monit. Assess.* **192**, 44. <https://doi.org/10.1007/s10661-019-7983-1> (2020).
18. Zhao, Q. H. *et al.* Landscape change and hydrologic alteration associated with dam construction. *Int. J. Appl. Earth Obs.* **16**(1), 17–26. <https://doi.org/10.1016/j.jag.2011.11.009> (2012).
19. Zhao, C. L. *et al.* Ecological security patterns assessment of Liao river basin. *Sustainability* **10**, 2401. <https://doi.org/10.3390/su10072401> (2018).
20. Yang, L. M. & Zhu, Z. L. The status quo and expectation of global and local land cover and land use RS research. *J. Nat. Resour.* **14**(4), 340–344 (1999).
21. Meyfroidt, P., Lambin, E. F., Erb, K. H. & Hertel, T. W. Globalization of land use: distant drivers of land change and geographic displacement of land use. *Curr. Opin. Env. Sust.* **5**(5), 438–444. <https://doi.org/10.1016/j.cosust.2013.04.003> (2013).
22. Forman, R. T. T. Some general principles of landscape and regional ecology. *Landscape Ecol.* **10**(3), 133–142. <https://doi.org/10.1007/BF00133027> (1995).
23. Xiao, D. N., Chen, W. B. & Guo, F. L. On the basic concepts and contents of ecological security. *Chin. J. Appl. Ecol.* **13**(3), 354–383. <https://doi.org/10.13287/j.1001-9332.2002.0084> (2002).
24. Gustafson, E. J., Roberts, L. J. & Leefers, L. A. Linking linear programming and spatial simulation models to predict landscape effects of forest management alternatives. *J. Environ. Manage.* **81**(4), 339–350. <https://doi.org/10.1016/j.jenvman.2005.11.009> (2006).
25. Restrepo, A. M. C. *et al.* Land cover change during a period of extensive landscape restoration in Ningxia Hui Autonomous Region China. *Sci Total Environ.* **598**, 669–679. <https://doi.org/10.1016/j.scitotenv.2017.04.124> (2017).
26. Gong, W. F. *et al.* Effect of terrain on landscape patterns and ecological effects by a gradient-based RS and GIS analysis. *J. For. Res.* **28**(5), 1061–1072. <https://doi.org/10.1007/s11676-017-0385-8> (2017).
27. Birhane, E. *et al.* Land use land cover changes along topographic gradients in Hugumburda national forest priority area, Northern Ethiopia. *Remote Sens. Appl. Soc. Environ.* **13**, 61–68. <https://doi.org/10.1016/j.rsase.2018.10.017> (2019).
28. Tian, P. *et al.* Research on land use changes and ecological risk assessment in Yangjiang River Basin in Zhejiang Province China. *Sustainability* **11**(10), 2817. <https://doi.org/10.3390/su11102817> (2019).

29. Xiong, M., Xu, Q. X. & Yuan, J. Analysis of multi-factors affecting sediment load in the Three Gorges Reservoir. *Quatern Int.* **208**, 76–84. <https://doi.org/10.1016/j.quaint.2009.01.010> (2009).
30. Feng, L. & Xu, J. Y. Farmers' willingness to participate in the next-stage Grain-for-Green project in the Three Gorges Reservoir Area China. *Environ. Manage.* **56**, 505–518. <https://doi.org/10.1007/s00267-015-0505-1> (2015).
31. Cao, S. *et al.* Ecosystem water imbalances created during ecological restoration by afforestation in China, and lessons for other developing countries. *J. Environ. Manage.* **183**, 843–849. <https://doi.org/10.1016/j.jenvman.2016.07.096> (2016).
32. Galicia, L., Zarco-Arista, A. E. & Mendoza-Robles, K. I. Land use/cover, landforms and fragmentation patterns in a tropical dry forest in the southern Pacific region of Mexico. *Singapore J. Trop. Geo.* **29**(2), 137–154. <https://doi.org/10.1111/j.1467-9493.2008.00326.x> (2008).
33. Zhong, S. Q. *et al.* Mechanized and optimized configuration pattern of crop-mulberry systems for controlling agricultural non-point source pollution on sloping farmland in the Three Gorges Reservoir Area, China. *Int. J. Env. Res. Pub. He.* **17**, 3599. <https://doi.org/10.3390/ijerph17103599> (2020).
34. Qi, S. W., Yue, Z. Q., Liu, C. L. & Zhou, Y. D. Significance of outward dipping strata in argillaceous limestones in the area of the Three Gorges reservoir China. *Bull. Eng. Geol. Environ.* **68**, 195–200. <https://doi.org/10.1007/s10064-009-0206-1> (2009).
35. Zhang, Q. *et al.* The spatial granularity effect, changing landscape patterns, and suitable landscape metrics in the Three Gorges Reservoir Area, 1995–2015. *Ecol. Indic.* <https://doi.org/10.1016/j.ecolind.2020.106259> (2020).
36. Yang, H. C., Wang, G. Q., Wang, L. J. & Zheng, B. H. Impact of land use changes on water quality in headwaters of the Three Gorges Reservoir. *Environ. Sci. Pollut. Res. Int.* **23**(12), 11448–11460. <https://doi.org/10.1007/s11356-015-5922-4> (2016).
37. Shen, Z. Y. *et al.* A comparison of WEPP and SWAT for modeling soil erosion of the Zhangjiachong Watershed in the Three Gorges Reservoir Area. *Agric. Water Manage.* **96**, 1435–1442. <https://doi.org/10.1016/j.agwat.2009.04.017> (2009).
38. Zhang, J. X., Liu, Z. J. & Sun, X. X. Changing landscape in the Three Gorges Reservoir Area of Yangtze River from 1977 to 2005: land use/land cover, vegetation cover changes estimated using multi-source satellite data. *Int. J. Appl. Earth Obs.* **11**, 403–412. <https://doi.org/10.1016/j.jag.2009.07.004> (2009).
39. Huang, C. B. *et al.* Land use/cover change in the Three Gorges Reservoir area, China: reconciling the land use conflicts between development and protection. *CATENA* **175**, 388–399. <https://doi.org/10.1016/j.catena.2019.01.002> (2019).
40. Wang, W. & Pu, Y. Analysis of landscape patterns and the trend of forest resources in the Three Gorges Reservoir area. *J. Geosci. Environ. Protect.* **6**, 181–192. <https://doi.org/10.4236/gep.2018.65015> (2018).
41. Li, Z., Wang, R., Zhou, Z. & Luo, X. Three Gorges Project's impact on the water resource and environment of Yangtze River. *J. Appl. Sci.* **13**(17), 3394–3399. <https://doi.org/10.3923/jas.2013.3394.3399> (2013).
42. Liang, X. Y. *et al.* Exploring cultivated land evolution in mountainous areas of Southwest China, an empirical study of development since the 1980s. *Land Degrad. Dev.* **32**, 546–558. <https://doi.org/10.1002/ldr.3735> (2021).
43. Kelly, M., Tuxen, K. A. & Stalberg, D. Mapping changes to vegetation pattern in a restoring wetland: Finding pattern metrics that are consistent across spatial scale and time. *Ecol. Indic.* **11**(2), 263–273. <https://doi.org/10.1016/j.ecolind.2010.05.003> (2011).
44. Guo, S. Q. *et al.* Spatiotemporal variation and landscape pattern of soil erosion in Qinling Mountains. *Chin. J. Ecol.* **38**(7), 2167–2176. <https://doi.org/10.13292/j.1000-4890.201907.016> (2019).
45. Peng, W. J. & Shu, Y. G. Analysis of landscape ecological security and cultivated land evolution in the Karst mountain area. *Acta Ecol. Sinc.* **38**(3), 852–865. <https://doi.org/10.5846/stxb201612062513> (2018).
46. Saura, S. Effects of remote sensor spatial resolution and data aggregation on selected fragmentation indices. *Landscape Ecol.* **19**(2), 197–209. <https://doi.org/10.1023/B:LAND.0000021724.60785.65> (2004).
47. Kerenyi, A. & Szabo, G. Human impact on topography and landscape pattern in the Upper Tisza region NE-Hungary. *Geogr. Fis. Din. Quat.* **30**(2), 193–196. <https://doi.org/10.1144/GSL.SP.2007.270.01.17> (2007).
48. Zhang, Y. X. *et al.* Changes in cultivated land patterns and driving forces in the Three Gorges Reservoir area, China, from 1992 to 2015. *J. Mt. Sci.* **17**(1), 203–215. <https://doi.org/10.1007/s11629-019-5375-1> (2020).
49. Teng, M. J. *et al.* Impacts of forest restoration on soil erosion in the Three Gorges Reservoir area China. *Sci. Total Environ.* **697**, 134164. <https://doi.org/10.1016/j.scitotenv.2019.134164> (2019).
50. He, L. H., King, L. & Tong, J. On the land use in the Three Gorges Reservoir area. *J. Geogr. Sci.* **13**(4), 416–422. <https://doi.org/10.1007/BF02837879> (2003).
51. Gao, J. M. *et al.* Bioavailability of organic phosphorus in the water level fluctuation zone soil and the effects of ultraviolet irradiation on it in the Three Gorges Reservoir China. *Sci. Total Environ.* **738**, 139912. <https://doi.org/10.1016/j.scitotenv.2020.139912> (2020).
52. Xie, Y. H. *et al.* The impact of Three Gorges Dam on the downstream eco-hydrological environment and vegetation distribution of East Dongting Lake. *Ecohydrology* **8**(4), 738–746. <https://doi.org/10.1002/eco.1543> (2015).
53. Cai, H. Y. *et al.* Quantifying the impact of the Three Gorges Dam on the thermal dynamics of the Yangtze River. *Environ. Res. Lett.* <https://doi.org/10.1088/1748-9326/aab9e0> (2018).
54. Tang, Q. *et al.* Flow regulation manipulates contemporary seasonal sedimentary dynamics in the reservoir fluctuation zone of the Three Gorges Reservoir China. *Sci. Total Environ.* **548**, 410–420. <https://doi.org/10.1016/j.scitotenv.2015.12.158> (2016).
55. Shen, Z. Y. *et al.* Assessment of nitrogen and phosphorus loads and casual factors from different land use and soil types in the Three Gorges Reservoir Area. *Sci. Total Environ.* **454–455**, 383–392. <https://doi.org/10.1016/j.scitotenv.2013.03.036> (2013).
56. Zhu, K. W. *et al.* Vegetation of the water-level fluctuation zone in the Three Gorges Reservoir at the initial impoundment stage. *Glob. Ecol. Conserv.* **21**, e00866. <https://doi.org/10.1016/j.gecco.2019.e00866> (2020).
57. Chen, C. D. *et al.* Restoration design for Three Gorges Reservoir shorelands, combining Chinese traditional agro-ecological knowledge with landscape ecological analysis. *Ecol. Eng.* **71**, 584–597. <https://doi.org/10.1016/j.ecoleng.2014.07.008> (2014).
58. Bao, Y., Gao, P. & He, X. The water-level fluctuation zone of Three Gorges Reservoir—a unique geomorphological unit. *Earth Rev.* **150**, 14–24. <https://doi.org/10.1016/j.earscirev.2015.07.005> (2015).
59. Li, Y. *et al.* Homogeneous selection dominates the microbial community assembly in the sediment of the Three Gorges Reservoir. *Sci. Total Environ.* **690**, 50–60. <https://doi.org/10.1016/j.scitotenv.2019.07.014> (2019).
60. Wang, L. J. *et al.* Role of reservoir construction in regional land use change in Pengxi River basin upstream of the Three Gorges Reservoir in China. *Environ. Earth Sci.* **75**, 1048. <https://doi.org/10.1007/s12665-016-5758-3> (2016).
61. Zhong, H. P. *et al.* Analysis of stage response of land use in Three Gorges Reservoir area: taking Hubei section of the reservoir area as an example. *J. Central Normal Univ. Nat. Sci.* **53**(4), 582–593. <https://doi.org/10.19603/j.cnki.1000-1190.2019.04.019> (2019).
62. Brady, N. C. & Weil, R. R. The nature and properties of Soils 14th. Prentice Hall, 2007:212–213.
63. Gerrard, J. Fundamentals of Soil: Berlin Germany: Routledge, 2000:110–115.
64. Otukey, J. R. & Blaschke, T. Land cover change assessment using decision trees, support vector machines and maximum likelihood classification algorithms. *Int. J. Appl. Earth Obs. Geoinf.* **12S**, S27–S31. <https://doi.org/10.1016/j.jag.2009.11.002> (2010).
65. Li, R. K., Li, Y. B., Wen, W. & Zhou, Y. L. Comparative study on spatial difference of elevation and slope in soil erosion evolution in typical watershed. *J. Soil Water Conserv.* **31**(5), 99–107. <https://doi.org/10.13870/j.cnki.stbxb.2017.05.016> (2017).
66. Li, S. F. *et al.* An estimation of the extent of cropland abandonment in mountainous regions of China. *Land Degrad. Dev.* **29**(5), 1327–1342. <https://doi.org/10.1002/ldr.2924> (2018).
67. Sang, X. *et al.* Intensity and stationarity analysis of land use change based on CART algorithm. *Sci. Rep-UK* **9**, 12279. <https://doi.org/10.1038/s41598-019-48586-3> (2019).

68. Strehmel, A., Schmalz, B. & Fohrer, N. Evaluation of land use, land management and soil conservation strategies to reduce non-point source pollution loads in the Three Gorges Region China. *Environ Manage* **58**, 906–921. <https://doi.org/10.1007/s00267-016-0758-3> (2016).
69. Liang, X. Y. *et al.* Traditional agroecosystem transition in mountainous area of Three Gorges Reservoir Area. *J Geogr Sci.* **30**(2), 281–296. <https://doi.org/10.1007/s11442-020-1728-5> (2020).
70. Kalerstagh, A. & Jeloudar, Z. J. Land use/cover change and driving force analyses in parts of northern Iran using RS and GIS techniques. *Arab. J. Geosci.* **4**(3–4), 401–411. <https://doi.org/10.1007/s12517-009-0078-5> (2011).
71. Ministry of Ecology and Environment of the People's Republic of China (MEE). Gazette of eco-environmental monitoring of three gorges project. Yangzi River, China 1997–2017 (in Chinese) (2018). <http://jcs.mep.gov.cn/hjzl/sxgb/2011sxgb/201206/P020120608565218279423.pdf>. Accessed 3 March 2019.
72. Xu, X. B. *et al.* Unravelling the effects of large-scale ecological programs on ecological rehabilitation of China's Three Gorges Dam. *J. Clean. Prod.* **256**, 120446. <https://doi.org/10.1016/j.jclepro.2020.120446> (2020).
73. Staged Assessment Group of Chinese Academy of Engineering (SAGCAE). Staged Assessment Report of the Three Gorges Project (Comprehensive Volume) (in Chinese). Chinese Water Power Press, Beijing, China (2010).
74. Li, R. K. *et al.* Study on the temporal and spatial variation of soil erosion intensity in typical watersheds of the Three Gorges Reservoir Area from 1988 to 2015: a case based on the Daning and Meixi River Watershed. *Acta Ecologica Sinica.* **38**(17), 6243–7257. <https://doi.org/10.5846/stxb201706071040> (2018).
75. Birhanu, L., Hailu, B. T., Bekele, T. & Demissew, S. Land use/land cover change along elevation and slope gradient in highlands of Ethiopia. *Remote Sensing Appl. Soc. Environ.* **16**, 100260 (2019).
76. Huang, X.Y., Ma, J.S. & Tang, Q. Introduction to geographic information systems. Beijing: Higher Education Press. 165–171 (2001).
77. Xiao, J. Y. *et al.* Evaluating urban expansion and land use change in Shijiazhuang, China, by using GIS and remote sensing. *Landscape Urban Plan.* **75**, 69–80. <https://doi.org/10.1016/j.landurbplan.2004.12.005> (2006).
78. Ye, Q. H. *et al.* Geospatial-temporal analysis of land-use changes in the Yellow River Delta during the last 40 years. *Sci China Ser D.* **47**, 1008–1024. <https://doi.org/10.1360/03yd0151> (2004).
79. Liu, J. Y. *The Land use in Xizang Autonomous Region* (Science Press, 1992).
80. Li, X. Z. *et al.* The adequacy of different landscape metrics for various landscape patterns. *Pattern Recogn.* **38**, 2626–2638. <https://doi.org/10.1016/j.patcog.2005.05.009> (2005).
81. Buyantuyev, A., Wu, J. G. & Gries, C. Multiscale analysis of the urbanization pattern of the Phoenix metropolitan landscape of USA: Time, space and thematic resolution. *Landscape Urban Plan.* **94**(3), 206–217. <https://doi.org/10.1016/j.landurbplan.2009.10.005> (2010).
82. McGarigal, K., Cushman, S.A. & Ene, E. FRAGSTATS v4: spatial pattern analysis program for categorical and continuous maps. Computer software program produced by the authors at the University of Massachusetts, Amherst. Preprint at <http://www.umass.edu/landeco/research/fragstats/fragstats.html> (2012).
83. Liu, X. L., Yang, Z. P., Di, F. & Chen, X. G. Evaluation on tourism ecological security in nature heritage sites—case of Kanas nature reserve of Xinjiang China. *Chin Geogra Sci.* **19**(3), 265–273. <https://doi.org/10.1007/s11769-009-026s5-z> (2009).
84. Zhang, R. S. *et al.* Landscape ecological security response to land use change in the tidal flat reclamation zone China. *Environ Monit Assess.* <https://doi.org/10.1007/s10661-015-4999-z> (2016).

Acknowledgements

This research is funded by the National Science and Technology Support Program of China (No. 2014BAC15B04), the National Natural Science Foundation of China (Nos. 42071228, 41261045, 41661020) and the Chongqing Research Program of Basic Research and Frontier Technology (Nos. cstc2015jcyjBX0128, cstc2018jcyjAX0539). The authors would like to thank the anonymous reviewers for their valuable comments.

Author contributions

R.L. conceived the methodology, data process and analyzed the results, Y.L. conducted the introduction and funding acquisition, B.L. analyzed the results and conclusions, D.F. participated in the design of the research framework and discussed the results analysis. All authors reviewed the manuscript.

Competing interests

The authors declare no competing interests.

Additional information

Correspondence and requests for materials should be addressed to B.L.

Reprints and permissions information is available at www.nature.com/reprints.

Publisher's note Springer Nature remains neutral with regard to jurisdictional claims in published maps and institutional affiliations.



Open Access This article is licensed under a Creative Commons Attribution 4.0 International License, which permits use, sharing, adaptation, distribution and reproduction in any medium or format, as long as you give appropriate credit to the original author(s) and the source, provide a link to the Creative Commons licence, and indicate if changes were made. The images or other third party material in this article are included in the article's Creative Commons licence, unless indicated otherwise in a credit line to the material. If material is not included in the article's Creative Commons licence and your intended use is not permitted by statutory regulation or exceeds the permitted use, you will need to obtain permission directly from the copyright holder. To view a copy of this licence, visit <http://creativecommons.org/licenses/by/4.0/>.

© The Author(s) 2021